On the Convergence and Accuracy of the Partition of Unity-based T3-CNS and T3-DNS Elements in Surface Fittings

Foek Tjong Wong[1][0000-0003-3628-8731] and Heri Istiono[2][0009-0002-7220-3846]

[1] Department of Civil Engineering, Petra Christian University, Surabaya 60236, Indonesia
[2] Doctoral Program of Civil Engineering, Petra Christian University, and Department of Civil Engineering, Adhi Tama Institute of Technology, Surabaya 60117, Indonesia
wftjong@petra.ac.id

Abstract. In recent years, several alternative non-standard finite element methods (FEMs) have been developed to improve the accuracy and convergence of the standard FEM. One of the proposed alternative FEMs which is of our interest is a method that combines the FEM and meshfree method using the partition of unity concept, called the three-node triangular element with continuous nodal stress (T3-CNS). In the T3-CNS element formulation, the shape functions are constructed using a combination of finite element continuous nodal gradient shape functions and a set of mesh-free shape functions obtained using the orthonormalized and constrained least-squares method. The aim of this paper is to present a numerical study on the accuracy and convergence of the T3-CNS interpolation when approximating several mathematically defined surfaces and their gradients. In addition, the discontinuous nodal stress version of the element, called the T3-DNS, is examined. The results are compared to those obtained using the standard triangular element and the Kriging-based triangular element. The results show that both the T3-CNS and T3-DNS interpolations possess the consistency property, providing highly accurate surface fittings, and exhibiting excellent convergence. Therefore, both the T3-CNS and T3-DNS interpolations are suitable to be employed as the trial function in numerical methods based on the Rayleigh-Ritz or Galerkin method.

Keywords: Partition of Unity, T3-CNS, T3-DNS, Surface Fitting; Orthonormalized and Constrained Least-squares Method.

1 Introduction

The finite element method (FEM) is a widely used numerical method for solving various engineering mathematical problems. In practice, FEM users prefer to use low-order elements such as three-node triangular elements and four-node quadrilateral elements. However, the accuracy of these low-order elements in predicting stresses (or other gradient fields) is low due to the discontinuity of the stresses over the element boundaries. Moreover, the accuracy of the elements is sensitive to the quality of the mesh, meaning that a distorted mesh can lead to less accurate results.

A class of alternative numerical methods referred to as the meshfree method has been of much interest since the early 1990s (refer to e.g. Liu [1] for an overview of the meshfree method). Compared to the traditional FEM, the meshfree method generally can produce more accurate and smoother stress fields. However, it also has a few weaknesses. For example, the essential boundary conditions in some formulations of the mesh-free method cannot be directly imposed as they lack the Kronecker delta property. Furthermore, the computational cost of the meshfree method is much higher compared to the FEM.

In recent years, researchers have proposed a class method that combines the benefits of the FEM and meshfree method, using the concept of partition of unity (PU). This method is referred to as the partition of unity-based FE-meshfree method (PU-based FE-meshfree) in this paper. In this method, the approximation function is a combination of a set of weight functions that sum to one over the problem domain, called the PU, and a local approximation function. Some examples of the PU-based FEM include the 'FE-Meshfree' quadrilateral element [2], the quadrilateral element with continuous nodal stress [3], the 'FE-Meshfree' triangular element [4], the three-node triangular element with continuous and discontinuous nodal stress (T3-CNS and T3-DNS) [5].

Among many proposed PU-based FE-meshfree methods, the T3-CNS and T3-DNS elements are of interest. The T3-CNS (T3-DNS) interpolation combines continuous nodal gradient (CNS) shape functions (conventional triangular shape functions (DNS)) as the PU and constrained orthonormalized least squares approximations as the local approximations. The T3-CNS and T3-DNS elements offer several advantages over the conventional triangular finite element. Firstly, they inherit the properties of high convergence rate and accuracy from the meshfree method. Secondly, they are less sensitive to mesh distortion than the standard triangular finite element. Furthermore, the T3-CNS element provides gradient continuity at the element nodes, resulting in a smooth global gradient field. Thus, these PU-based triangular elements are good alternatives to the classical finite elements.

The T3-CNS and T3-DNS elements were originally developed in linear static plane elasticity problems [5]. Subsequently, they have been applied to the free vibration of plane elasticity models [6] and geometric nonlinear solid mechanic problems [7]. However, previous works have not examined the accuracy and convergence of the T3-CNS and T3-DNS interpolations in approximating mathematically defined surfaces. Therefore, this paper aims to present a numerical study on the consistency, accuracy, and convergence of the T3-CNS and T3-DNS interpolations and their derivatives in surface fittings. This study is based on the approach of Wong *et al.* [8]. It aims to provide valuable insights into the interpolation characteristics of the T3-CNS and T3-DNS elements, which could be used as the trial solution in a Galerkin or Rayleigh-Ritz method for solving a boundary value problem related to practical engineering applications.

2 T3-CNS and T3-DNS Interpolations

Similar to the standard FEM, to construct the T3-CNS or T3-DNS interpolation, a two-dimensional problem domain Ω is partitioned using a mesh of three-node triangular elements, Ω^h. The approximation of a surface function $z = z(x, y)$ (or other field variables) over a typical triangular element $\bar{\Omega}^e \subset \Omega^h$ is given as

$$z \approx z^h = \sum_{i=1}^{3} w_i(L_1, L_2, L_3) z_i(x, y) \tag{1}$$

where $w_i(L_1,L_2,L_3)$ is the weight function associated with node i, expressed in terms of the triangular area coordinates L_1, L_2, and L_3, and $z_i(x, y)$ is the local approximation centered at node i. The T3-CNS weight functions are given as [5]:

$$w_1 = L_1 + L_1^2 L_2 + L_1^2 L_3 - L_1 L_2^2 - L_1 L_3^2 \tag{2}$$

$$w_2 = L_2 + L_2^2 L_3 + L_2^2 L_1 - L_2 L_3^2 - L_2 L_1^2 \tag{3}$$

$$w_3 = L_3 + L_3^2 L_1 + L_3^2 L_2 - L_3 L_1^2 - L_3 L_2^2 \tag{4}$$

Theses weight functions and their first derivatives are continuous at the element nodes. However, along the element boundaries, only the functions are continuous (i.e., C^0 continuous). On the other hand, the T3-DNS weight functions are adopted from the shape functions of the standard three-node triangular element. The T3-DNS shape functions are continuous at every point along the element boundaries but their derivatives are not continuous.

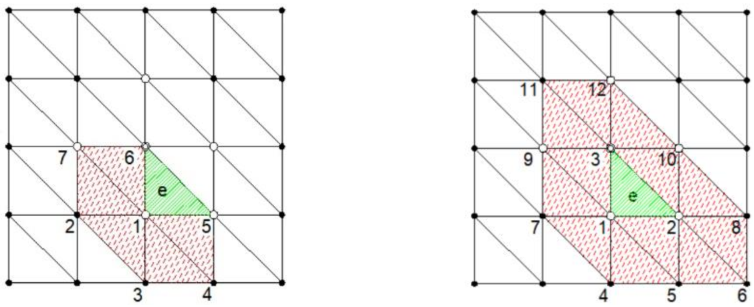

Fig. 1. (a) Support of node 1 of element no. *e* is the shaded area around node 1; (b) Support of element no. *e* is the shaded area around element *e*, including the element *e* itself.

The nodal approximation $z_i(x, y)$ is established using a constrained and orthonormalized least squares (CO-LS) method, which was first introduced by Tang *et al*. [3]. To construct the CO-LS approximation, the supports of node i, $\bar{\Omega}_i$ $i = 1, 2, 3$, are defined as the region around node i encompassing all the elements that share node i. Node i is called the central node whereas the other connected nodes are called satellite nodes. For example, Fig. 1(a) shows the support of node 1 of element no. *e* encompassing six triangular elements that share node 1 (the central node), covering six satellite nodes, namely, 2, 3, 4, 5, 6, and 7.

Consider a nodal support $\overline{\Omega}_i$ with n supporting nodes. Let the numbering labels for the nodes in the support be j, j = 1, …, n. The CO-LS approximation around node i can be written as

$$z_i(x,y) = \mathbf{\Phi}_i(x,y)\mathbf{z}_i = \sum_{j=1}^{n} \phi_j^{[i]}(x,y) z_j \tag{5a}$$

$$\mathbf{\Phi}_i(x,y) = \begin{bmatrix} \phi_1^{[i]}(x,y) & \phi_2^{[i]}(x,y) & \cdots & \phi_n^{[i]}(x,y) \end{bmatrix} = \mathbf{r}^{\mathrm{T}}(x,y)\mathbf{B}^{[i]} \tag{5b}$$

where $\varphi_j^{[i]}(x, y)$ is the CO-LS shape function for nodal approximation of node i, associated with node j, and the vector

$$\boldsymbol{z}_i = \{z_1 \quad z_2 \quad \cdots \quad z_n\}^T \tag{6}$$

is the $n\times1$ vector of nodal values z_j at the supporting nodes. The vector $\mathbf{r}(x, y)$ is the orthonormalized polynomial bases vector obtained by transforming a polynomial bases vector $\mathbf{p}(x, y)$ in such a way to make the moment matrix in the least squares procedure becomes an identity matrix [9]. In this study, the basis function used is a quadratic polynomial, viz.

$$\mathbf{p}(x,y) = [1 \quad x \quad y \quad x^2 \quad xy \quad y^2]^{\mathrm{T}} \tag{7}$$

The matrix $\mathbf{B}^{[i]}$ is defined as follows:

$$\mathbf{B}^{[i]} = \begin{bmatrix} \mathbf{B}_1^{[i]} & \mathbf{B}_2^{[i]} & \cdots & \mathbf{B}_n^{[i]} \end{bmatrix} \tag{8a}$$

$$\mathbf{B}_j^{[i]} = \mathbf{r}(x_j, y_j) - f_j^{[i]}\mathbf{r}(x_i, y_i) \tag{8b}$$

$$f_j^{[i]} = \begin{cases} \dfrac{\mathbf{r}^{\mathrm{T}}(x_i,y_i)\mathbf{r}(x_j,y_j)}{\mathbf{r}^{\mathrm{T}}(x_i,y_i)\mathbf{r}(x_i,y_i)} & \text{if } j \neq i \\ \dfrac{\mathbf{r}^{\mathrm{T}}(x_i,y_i)\mathbf{r}(x_j,y_j)-1}{r^{T}(x_i,y_i)r(x_i,y_i)} & \text{if } j = i \end{cases} \tag{8c}$$

It is worth noting that the number of nodes in the nodal support, n, may be not the same for each i = 1, 2, 3.

To combine the weighting functions $w_i(L_1,L_2,L_3)$, i = 1, 2, 3, and the CO-LS shape functions $\varphi_j^{[i]}$, j = 1, 2, ..., n, we define the support of element no. e, $\widehat{\Omega}^e$, as the union of the four nodal supports: $\widehat{\Omega}^e = \overline{\Omega}_1 \cup \overline{\Omega}_2 \cup \overline{\Omega}_3$. Let the nodal numbering labels in the element support $\widehat{\Omega}^e$ be I = 1, 2, ..., N, where N is the total number of nodes in the element support. For example, Fig. 1(b) shows the support of element no. e, which covers 12 nodes (N = 12). Referring to this element numbering system and substituting Eq. (5a) into Eq. (1), the approximate surface function can be expressed as

$$z^h = \sum_{I=1}^{N} \psi_I(x,y) z_I \tag{9a}$$

$$\psi_I(x,y) = \sum_{i=1}^{3} w_i(L_1,L_2,L_3)\, \phi_I^{[i]}(x,y) \tag{9b}$$

where $\psi_I(x, y)$ is the T3-CNS or T3-DNS shape function associated with node I. In Eq. (9b), if node I is not in the nodal support of node i, then $\varphi_I^{[i]}$ is defined to be zero. It is apparent that the T3-CNS or T3-DNS shape function is a linear combination of the weighting functions and the CO-LS shape functions.

3 Numerical Tests

Several numerical tests are conducted to assess the accuracy and convergence of the T3-CNS and T3-DNS interpolations and their derivatives on surface fittings of $z = f(x, y)$. The approximation error is measured using the relative L_2 norm of error, that is,

$$r_z = \sqrt{\frac{\int_{\Omega^h} (z^h - z)^2 dA}{\int_{\Omega^h} z^2 dA}} \tag{10}$$

where z is the surface function under consideration. This error norm is also used to measure the relative error of the partial derivatives of the function (by replacing z and z^h with their derivatives). The integral in Eq. (10) is evaluated numerically using the Gaussian quadrature rule for triangular elements with the six-quadrature rule. The results are then compared to those obtained using the standard triangular element (T3) and the Kriging-based triangular element with a quadratic basis, two layers of elements, and the quartic spline correlation function (K-T3) [10][11].

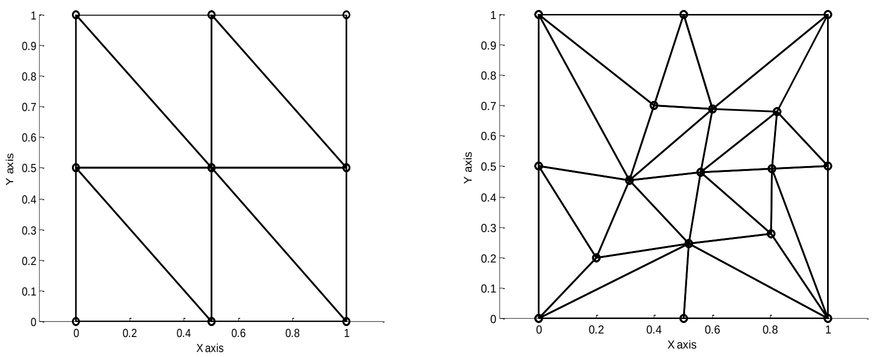

(a) Regular mesh (b) Irregular mesh

Fig. 2. Square function domain with (a) a regular mesh of triangular elements and (b) an irregular mesh of triangular elements.

3.1 Consistency Property

An interpolation scheme that can represent exactly all polynomial terms of degree m is called m-consistent. As a quadratic polynomial basis is used in this study to construct the T3-CNS and T3-DNS interpolations, they are expected to reproduce quadratic functions. To examine their consistency property, we employed a unit square domain, which was partitioned into a regular and an irregular mesh of triangular elements, as shown in

Fig. 2(a) and Fig. 2(b), respectively. The functions considered were the bases of a quadratic polynomial, that is, $z = 1$, $z = x$, $z = y$, $z = x^2$, $z = xy$ and $z = y^2$.

The numerical results show that the relative errors for the T3-CNS and T3-DNS interpolations and their derivatives with respect to the variables x and y are on the order of 10^{-15} to 10^{-16}. These errors are merely due to computer round-off errors. Thus, the T3-CNS and T3-DNS interpolations are found to have the quadratic consistency property. In comparison, the K-T3 interpolation is also observed to be quadratic consistent. The T3 interpolation, however, is only able to reproduce exact solutions up to the linear basis functions (linear consistent).

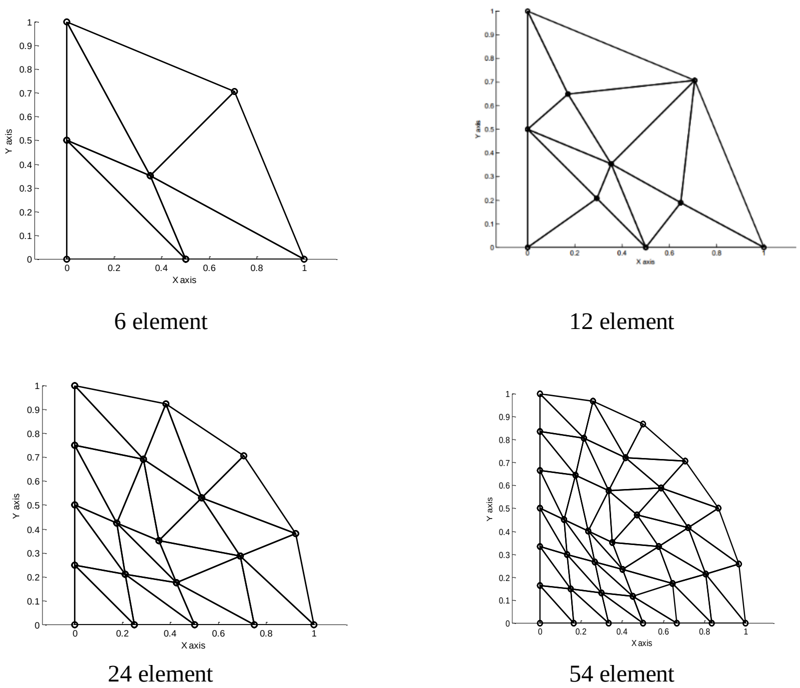

Fig. 3. A quarter-circular function domain divided into triangular elements.

3.2 Accuracy and Convergence

To examine the accuracy and convergence of the T3-CNS and T3-DNS interpolations in surface fittings, we use a bi-cosine function (adopted from Wong *et al.* [8])

$$z = \cos(\frac{\pi}{2}x)\cos(\frac{\pi}{2}y) \tag{11}$$

defined over two different domains, namely,

$$\widehat{\Omega}_S = \{(x, y)|0 \leq x \leq 1, 0 \leq y \leq 1\} \tag{12}$$

$$\widehat{\Omega}_C = \{(x, y) | x^2 + y^2 \leq 1, x \geq 0, y \geq 0\} \quad (13)$$

Eq. (12) represents a unit square while Eq. (13) represents a quarter of a unit circle. The unit square is partitioned using regular triangular meshes of 2×2 (Fig (2.a)), 4×4, 8×8 and 16×16. On the other hand, the quarter circle is partitioned using triangular meshes of 6, 12, 24, and 54 elements as shown in Fig. 3.

The resulting relative errors of the T3-CNS and T3-DNS interpolations and other comparative interpolations are presented in Table 1 for the circular domain. The results for the square domain are not presented here due to space limitations. The results for both square and circular function domains show that the T3-CNS and T3-DNS interpolations give reasonably accurate surface approximations and converge well as the mesh is refined. The accuracy and convergence of T3-CNS, T3-DNS, and K-T3 interpolations are similar with no significant differences. The T3 interpolation results, however, are much less accurate than the other interpolations.

Table 1. Relative errors (%) of the approximation of the bi-cosine function, r_z, and its partial derivatives, $r_{z,x}$ and $r_{z,y}$ over the unit circular domain.

Mesh		r_z		
# element	T3-CNS	T3-DNS	K-T3	T3
6	4.99	4.99	4.7	13.18
12	2.84	2.82	2.66	6.48
24	0.85	0.84	0.75	3.55
54	0.22	0.22	0.15	1.55

Mesh		$r_{z,x}$		
# element	T3-CNS	T3-DNS	K-T3	T3
6	12.2	12.14	12.35	43.31
12	10.35	9.92	10.85	28.47
24	4.83	4.53	4.25	20.91
54	2.18	1.93	1.46	13.68

Mesh		$r_{z,y}$		
# element	T3-CNS	T3-DNS	K-T3	T3
6	8.33	8.28	12.35	29.56
12	9.89	9.51	10.79	27.99
24	3.47	3.25	4.25	15.01
54	1.6	1.44	1.49	10.01

While the accuracy and convergence of the T3-CNS and T3-DNS interpolations are similar to those of the K-T3 interpolation in surface fitting problems, the former ones are continuous over interelement boundaries (constitute conforming elements) whereas the latter is discontinuous over interelement boundaries (constitute nonconforming elements) [10]. This discontinuity may affect negatively to the convergence rate of solutions in the context of C^0 continuum models such as the plane elasticity [10].

4 Conclusions

A series of numerical tests have been conducted to assess the consistency property, accuracy, and convergence of the T3-CNS and T3-DNS interpolations. The results show that they are quadratic consistent for both irregular and irregular meshes, which is also true for the K-T3 interpolation. However, the T3 interpolation can only achieve consistency up to a linear function. The accuracy and convergence of the T3-CNS and T3-DNS interpolations are similar to those of the K-T3 interpolation. The advantage of the T3-CNS and T3-DNS over the K-T3 is their continuity over interelement boundaries. The T3-CNS and T3-DNS interpolation accuracy is significantly better than the standard triangular element interpolation. Hence, the T3-CNS and T3-DNS interpolations are viable alternatives to be used in Rayleigh-Ritz or Galerkin-based numerical methods for solving C^0 continuum problems related to practical engineering applications.

References

1. Liu, G. R.: An overview on meshfree methods. International Journal of Computational Methods 13(5), 1630001-1–1630001-42 (2016).
2. Rajendran, S., Zhang, B. R.: A “FE-Meshfree” QUAD4 element based on partition of unity. Computer Methods in Applied Mechanics and Engineering 197(1–4), 128–147 (2007).
3. Tang, X. H., Zheng, C., Wu, S. C., Zhang, J. H.: A novel four-node quadrilateral element with continuous nodal stress. Applied Mathematics and Mechanics (English Edition) 30(12), 1519–1532 (2009).
4. Xu, J. P., Rajendran, S.: A ‘FE-Meshfree’ TRIA3 element based on partition of unity for linear and geometry nonlinear analyses. Computational Mechanics 51, 843–864 (2013).
5. Yang, Y., Tang, X., Zheng, H.: A three-node triangular element with continuous nodal stress. Computers and Structures 141, 46–58 (2014).
6. Yang, Y., Xu, D., Zheng, H.: Application of the three-node triangular element with continuous nodal stress for free vibration analysis. Computers and Structures 169, 69–80 (2016).
7. Sun, G., Yang, Y., Zheng, H.: A three-node triangular element with continuous nodal stress for geometry nonlinear solid mechanics problems. International Journal of Computational Methods 15(04), 1850022 (2017).
8. Wong, F. T., Soetanto, R., Budiman, J.: On the accuracy and convergence of the hybrid FE-meshfree Q4-CNS element in surface fitting problems. MATEC Web of Conferences 147, 01002, 1–7 (2018).
9. Zheng, C., Tang, X. H., Zhang, J. H., Wu, S. C.: A novel mesh-free poly-cell Galerkin method. Acta Mechanica Sinica 25(4), 515–527 (2009).
10. Wong, F. T., Kanok-Nukulchai, W: On the convergence of the Kriging-based finite element method. International Journal of Computational Methods 06(01), 93–118 (2009).
11. Wong, F. T., Kanok-Nukulchai, W: Kriging-based finite element method: Element-by-element Kriging Interpolation. Civil Engineering Dimension 11(1), 15–22 (2009).